PHOTONICS Research

Effects of background spectral noise in the phase-modulated single-frequency seed laser on high-power narrow-linewidth fiber amplifiers

Wei Liu,[1] Jiaxin Song,[1] Pengfei Ma,[1,2] Hu Xiao,[1] and Pu Zhou[1,3]

[1]College of Advanced Interdisciplinary Studies, National University of Defense Technology, Changsha 410073, China
[2]e-mail: shandapengfei@126.com
[3]e-mail: zhoupu203@163.com

Received 4 November 2020; revised 10 January 2021; accepted 18 January 2021; posted 19 January 2021 (Doc. ID 414223); published 2 March 2021

In this work, we analyze the effects of the background spectral noise in phase-modulated single-frequency seed lasers on the spectral purity of high-power narrow-linewidth fiber amplifiers. Through demonstrating the spectral evolution of the phase-modulated single-frequency part and the background spectral noise in a narrow-linewidth fiber amplifier, the mechanism for the spectral wing broadening effect is clarified and design strategies to maintain high spectral purity are given. Specifically, the background spectral noise in phase-modulated single-frequency seed lasers could lead to obvious spectral wing broadening and degeneration of spectral purity in narrow-linewidth fiber amplifiers through the four-wave-mixing effect. Notably, the spectral wing broadening effect could be suppressed by filtering out the background spectral noise in the seed laser or applying a counter-pumped configuration in the fiber amplifier. We have also conducted contrast experiments, which have verified the validity of the theoretical model and the design strategies for high-spectral-purity operation.

https://doi.org/10.1364/PRJ.414223

1. INTRODUCTION

High-power fiber lasers have been highly desired for many industrial and scientific applications, including material processing, manufacturing, nonlinear conversion, and gravitational-wave detection [1–4]. Unfortunately, power scaling of a single monolithic fiber laser system is currently limited by the optical nonlinearities, optical damage, and transverse mode instability [5–9]. Coherent beam combining and spectral beam combining provide two effective approaches to further improve the output power of fiber lasers while maintaining excellent beam quality [10–13]. The key unit in the two beam combining systems is the high-power narrow-linewidth fiber amplifier. The properties of the high-power narrow-linewidth fiber amplifier, especially for the output power and spectral purity, tightly determine the performances of the two beam combining systems. However, it is challenging to realize high power and high spectral purity simultaneously due to the inevitable spectral broadening effect in high-power fiber amplifiers.

Different types of narrow-linewidth seed sources have been applied in high-power fiber amplifiers for narrow-linewidth operation, including filtered superfluorescent fiber sources [13], random distributed feedback fiber lasers [14], fiber-Bragg-grating-stabilized laser diodes [15], multi-longitudinal fiber oscillators [16–18], and phase-modulated single-frequency lasers [19–21]. Those seed sources could be classified into two categories according to the strategies for narrow-linewidth operation. One is to apply the seed source with narrower spectral linewidth as much as possible and to optimize the fiber amplifier to avoid the impact of the spectral broadening [13–18]. The other is to control the spectral broadening effect through applying a seed source with stable intensity [19–21]. Despite that higher than kilowatt-level narrow-linewidth fiber amplifiers with diffraction-limited beam quality have been reported based on the above two categories, the extensibility of the first one is limited because the seed laser with a narrower spectral linewidth might lead to more serious issues of nonlinear effects and the spectral broadening effect [22,23]. Accordingly, most of the reported high-power narrow-linewidth fiber amplifiers are based on phase-modulated single-frequency seed lasers [24–27], which naturally have stable intensity and can maintain the spectral linewidth during amplification. However, there could also exist obvious spectral wing broadening in those narrow-linewidth fiber amplifiers based on phase-modulated single-frequency seed lasers [25,26], which would decrease the spectral purity of the output laser and degrade their performance in further applications.

In this work, we aim to clarify the mechanism of the spectral wing broadening effect in narrow-linewidth fiber amplifiers based on phase-modulated single-frequency seed lasers and

propose possible techniques to suppress this phenomenon. Through investigating the effects of background spectral noise in the phase-modulated single-frequency seed laser on the spectral evolution in the Yb-doped fiber amplifier (YDFA), we propose a spectral evolution model for the phase-modulated single-frequency part and the background spectral noise in narrow-linewidth fiber amplifiers. The mechanism for the spectral wing broadening effect is clarified, and design strategies to maintain high spectral purity are given according to the theoretical analysis. We have also conducted contrast experiments to verify the theoretical model and the design strategies for high-spectral-purity operation.

2. THEORY FOR NUMERICAL MODELING

The phase-modulated single-frequency laser is commonly based on a single-frequency laser, which is externally modulated through an electro-optic modulator to broaden its linewidth to effectively suppress the stimulated Brillouin scattering (SBS) effect. Therefore, the phase-modulated single-frequency laser could have stable intensity and maintain its spectral shape during amplification. Accordingly, the obvious spectral wing broadening effect in a high-power narrow-linewidth fiber amplifier based on phase-modulated single-frequency seed laser indicates that additional noise is introduced into the seed laser. One strong possibility for this noise source is the background spectral noise, which could originate from the amplified spontaneous emission noise in the preamplifiers. To demonstrate the possible impact of the background spectral noise in the phase-modulated single-frequency seed laser on the spectral evolution in the high-power narrow-linewidth YDFA, we need to construct a phase-modulated single-frequency seed laser with background spectral noise and describe the spectral evolution of the total seed laser in the YDFA. There exist two different spectral components in the total seed laser: the phase-modulated single-frequency part and the background spectral noise. Accordingly, it is preferable to analyze the spectral evolution of the total seed laser through separate descriptions of the two different spectral components (two seed lasers). Then both the output properties of the total signal laser and the interactions between the two different spectral components could be included in the theoretical analysis.

As for the spectral evolution of a single seed laser in a YDFA, it could be generally divided into two main energy conversion processes, i.e., the energy absorption from pump laser to signal laser and the energy conversion among different spectral components. Consequently, the basic approach to model the spectral evolution of a single seed laser in a YDFA is the joint analysis of the two energy conversion processes. Specifically, the two energy conversion processes could be described through the rate equation and the nonlinear propagation equation. When it comes to the case of two seed lasers, the interactions between the two seed lasers could also lead to energy conversion between them. Accordingly, the effects, such as gain competition, cross-phase modulation (XPM), and four-wave mixing (FWM), should also be included in the rate equation and the nonlinear propagation equation. Then the set of unidirectional spectral-spatial equations describing the spectral evolutions of two spectral components in a YDFA could be expressed as

$$\frac{N_2}{N_0}=\frac{\frac{\Gamma_p}{\omega_p A_e}\sigma_p^a P_p+\frac{1}{2\pi T_m A_e}\int\frac{\Gamma_s}{\omega}\sigma_\omega^a(|\tilde{A}_0|^2+|\tilde{A}_1|^2)\mathrm{d}\omega}{\frac{\Gamma_p}{\omega_p A_e}(\sigma_p^a+\sigma_p^e)P_p+\frac{1}{\tau}+\frac{1}{2\pi T_m A_e}\int\frac{\Gamma_s}{\omega}(\sigma_\omega^a+\sigma_\omega^e)(|\tilde{A}_0|^2+|\tilde{A}_1|^2)\mathrm{d}\omega}, \tag{1}$$

$$\frac{\mathrm{d}P_p}{\mathrm{d}z}=\Gamma_p(\sigma_p^e N_2-\sigma_p^a N_1)P_p-\alpha_p P_p, \tag{2}$$

$$\frac{\partial\tilde{A}_0}{\partial z}=\frac{1}{2}\Gamma_s(\sigma_s^e N_2-\sigma_s^a N_1)\tilde{A}_0-\frac{\alpha_s}{2}\tilde{A}_0+\frac{i}{2}\beta_2\omega^2\tilde{A}_0 + i\gamma F\{(|A_0|^2+2|A_1|^2)A_0+A_1A_1A_0^*\}, \tag{3}$$

$$\frac{\partial\tilde{A}_1}{\partial z}=\frac{1}{2}\Gamma_s(\sigma_s^e N_2-\sigma_s^a N_1)\tilde{A}_1-\frac{\alpha_s}{2}\tilde{A}_1+\frac{i}{2}\beta_2\omega^2\tilde{A}_1 + i\gamma F\{(|A_1|^2+2|A_0|^2)A_1+A_0A_0A_1^*\}, \tag{4}$$

where the subscripts p and s stand for pump laser and signal laser, respectively; the subscripts 0 and 1 stand for the phase-modulated single-frequency part and the background spectral noise; $\tilde{A}$ and A are the envelope of the signal field in the spectral and temporal versions; σ^a and σ^e are the corresponding absorption and emission cross sections; N_1 and N_2 are the ion densities in the ground state or excited state; $N_1+N_2=N_0$; N_0 is the dopant density in the fiber core; Γ is the power overlap factor; $\hbar$ is the Planck constant; ω is the angular frequency; A_e is the effective mode area of the fiber; τ is the lifetime of the excited state; T_m is the time window during the calculation; α is the loss coefficient; β_2 is the second-order dispersion coefficient; γ is the nonlinear coefficient; and $F\{\}$ denotes the Fourier transform. Equations (1)–(4) describe the evolutions of the ion density in the excited state N_2, the pump power P_p, the spectral envelope of the phase-modulated single-frequency part $\tilde{A}_0$, and the spectral envelope of the background spectral noise $\tilde{A}_1$ along the fiber, respectively. An iterative solution of Eqs. (1)–(4) is obtained numerically using the Runge–Kutta method with the initial conditions.

To apply the above equations to describe the spectral evolution in a YDFA, we first construct the initial inserted seed lasers separately, including the phase-modulated single-frequency part and the background spectral noise. As for the phase-modulated single-frequency part, its spectral shape could be controlled by adjusting the phase modulation signal. Without loss of generality, we apply the commonly used white noise modulation to construct the phase-modulated single-frequency part. Figures 1(a) and 1(b) illustrate the normalized temporal and spectral intensity of the constructed

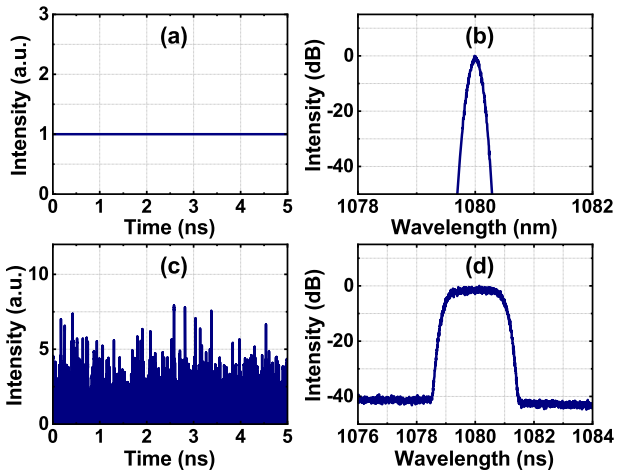

Fig. 1. Normalized temporal and spectral intensity of the constructed phase-modulated single-frequency part (first line) and background spectral noise (second line): (a), (c) normalized temporal intensity; (b), (d) normalized spectral intensity.

phase-modulated single-frequency part. As shown in Fig. 1(a), the intensity of the phase-modulated single-frequency part remains stable in a nanosecond time scale. As shown in Fig. 1(b), the spectral shape of the phase-modulated single-frequency part is close to Gaussian, and the corresponding full width at half-maximum (FWHM) spectral linewidth is about 0.1 nm. As for the background spectral noise, it usually originates from the spontaneous emission noise and could have similar properties to the amplified spontaneous emission source. Thus, we construct the background spectral noise based on the filtered amplified spontaneous emission source obtained from the simplified propagation equation [28] and adjust the spectral shape of the background spectral noise through changing the spectrum of the filter. Figures 1(c) and 1(d) illustrate the normalized temporal and spectral intensity of the constructed background spectral noise, when the spectral shape and the bandwidth of the filter are set to be super-Gaussian and 2.0 nm, respectively. As shown in Fig. 1(c), there exist strong intensity fluctuations in the nanosecond time scale for the constructed background spectral noise, and the maximum power of the constructed background spectral noise is over 8 times that of the mean power. As shown in Fig. 1(d), the spectral shape of the constructed background spectral noise is close to rectangular, and the FWHM spectral linewidth is about 2.0 nm.

3. SIMULATION RESULTS

Based on the spectral evolution model and the constructed initial inserted seed lasers, we simulate the spectral evolutions of both the phase-modulated single-frequency part and the background spectral noise for a typical co-pumped high-power narrow-linewidth fiber amplifier. Here we set the power ratio and bandwidth of the background spectral noise to be −30 dB and 2 nm, respectively. The major simulation parameters of the fiber amplifier are shown in Table 1. The core and inner cladding diameters of the YDF are 20 μm and 400 μm, respectively. The

Table 1. Major Simulation Parameters for the Fiber Amplifier

Parameter	Value	Parameter	Value
λ_p	976 nm	λ_s	1080 nm
α	1.5 dB/km	γ	0.5 W^{-1}/km
Γ_p	0.0025	Γ_s	0.85
L_{act}	15 m	L_{pas}	1 m
τ	0.84 ms	N	7.8×10^{25}
σ_p^a	1.77×10^{-24} m^2	σ_p^e	1.71×10^{-24} m^2
σ_s^a	2.29×10^{-27} m^2	σ_s^e	2.82×10^{-25} m^2
β_2	12 ps^2/km	P_{seed}	50 W
dt	1×10^{-13} s	T_{max}	5×10^{-8} s

absorption coefficient of the initial pump laser is set to be about 1.5 dB/m. For simplicity, the loss coefficient is set to be the same at different wavelengths, and the insertion loss of the pump laser is omitted. Due to our main purpose being to investigate the spectral evolution of the fiber amplifier, not power scaling limitations, we ignore the SBS and stimulated Raman scattering (SRS) effects and focus on a case well below the SBS and SRS thresholds.

A. Properties of the Fiber Amplifier at Different Pump Powers

Figures 2(a) and 2(b) illustrate the output powers and spectra of the total signal laser at different pump powers when the phase-modulated single-frequency seed laser with background spectral noise is applied as the total seed laser. As shown in Fig. 2(a), the

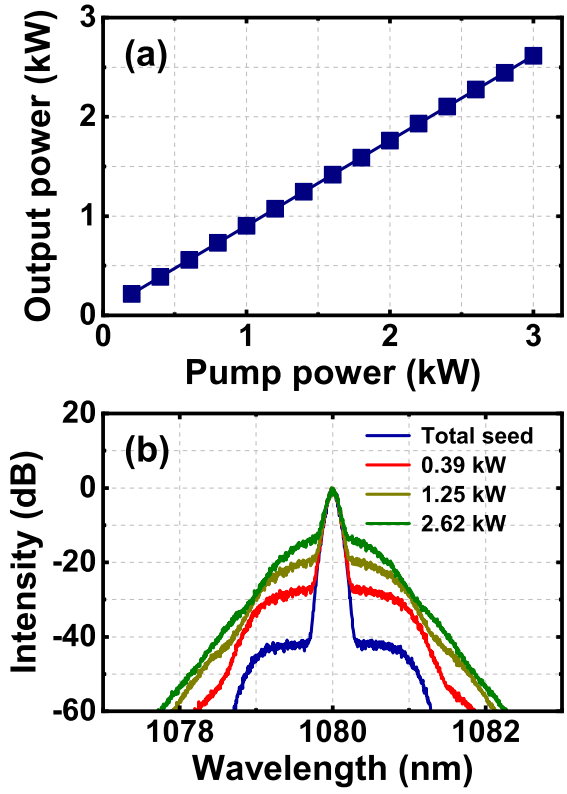

Fig. 2. Output powers and spectra of the total signal laser at different pump powers: (a) output power; (b) output spectra.

output power of the total signal laser grows almost linearly with the pump power, and the corresponding slope efficiency is about 86%. Thus, the background spectral noise in the seed laser would not impact the slope efficiency of the fiber amplifier. As shown in Fig. 2(b), the central spectra of the total signal laser remain nearly unchanged compared to that of the total seed laser, while there exists an obvious spectral wing broadening phenomenon with increasing output power.

To give a more quantitative description of this spectral wing broadening effect and its impact on the spectral purity, we have calculated the corresponding power-ratio spectral linewidth of the total signal laser. Here, the power-ratio spectral linewidth is defined as the minimum spectral linewidth within which the power ratio of the signal laser is over a certain proportion. Figure 3 illustrates the power-ratio spectral linewidths of the total signal laser at different output powers. As for the 80% power-ratio spectral linewidth, it grows gradually from about 0.16 nm to about 0.32 nm when the output power increases from 0.22 to 2.62 kW. As for the 90% power-ratio spectral linewidth, it grows steadily from 0.21 nm to about 0.31 nm when the output power is below 1.42 kW, and it grows quickly to about 0.75 nm at an output power of 2.62 kW. As for the 99% power-ratio spectral linewidth, it grows quickly from 0.35 nm to about 1.24 nm when the output power increases to about 0.73 kW, and it continues to grow to about 1.64 nm at an output power of 2.62 kW. This spectral broadening saturation phenomenon for the 99% power-ratio spectral linewidth is related to the bandwidth of background spectral noise, which is set to be 2 nm in the simulation. Despite the spectral wing broadening phenomenon, most of the energy in the background spectral noise would remain within the bandwidth of 2 nm. Thus, when the 99% power-ratio spectral linewidth of the total signal laser becomes comparable to the original bandwidth of the background spectral noise, the spectral wing broadening effect begins to saturate. It should be noted that the 80%, 90%, and 99% power-ratio spectral linewidths of the total seed laser are about 0.16, 0.21, and 0.33 nm, respectively. Thus, the corresponding spectral broadening factors are about 2.0, 3.6, and 5.0, respectively, at an output power of 2.62 kW. Accordingly, the spectral wing broadening effect corresponds to the growth of the power-ratio spectral linewidth and the decrease of the spectral purity. Therefore, it might be concluded that the background spectral noise in the phase-modulated single-frequency seed laser would lead to obvious spectral wing broadening and degrade the spectral purity of narrow-linewidth fiber lasers.

B. Mechanism for the Spectral Wing Broadening

To demonstrate the mechanism for the spectral wing broadening effect, we investigate the interactions between the phase-modulated single-frequency part and the background spectral noise in the total seed laser during amplification. Figure 4 illustrates the power evolutions of the two spectral components along the fiber amplifier at a pump power of 2 kW. As shown in Fig. 4, both the central part and the background spectral noise become amplified along the fiber. The powers of the central phase-modulated single-frequency part and the background spectral noise at the output port are about 1.51 kW and 0.25 kW, respectively. The corresponding power ratio of the background spectral noise increases from −30 dB to about −8.7 dB during power amplification. Accordingly, the background spectral noise gets extra amplification compared to the central phase-modulated single-frequency part.

Figures 5(a) and 5(b) illustrate the normalized spectral evolutions of the two spectral components along the fiber amplifier at a pump power of 2 kW. As shown in Fig. 5(a), the central spectrum of the phase-modulated single-frequency part remains nearly unchanged at different positions along the fiber amplifier, while the spectral wing begins to be enhanced after the fiber length of about 7.5 m. As shown in Fig. 5(b), the spectrum of the background spectral noise begins to concentrate after the fiber length of about 5 m. Accordingly, the spectrum of the phase-modulated single-frequency part broadens while the spectrum of the background spectral noise concentrates after amplification, which indicates that energy conversion might occur between the phase-modulated single-frequency part and background spectral noise.

The two spectral components have similar spectral bands, and the power ratio of the background spectral noise is much lower than that of the phase-modulated single-frequency part in

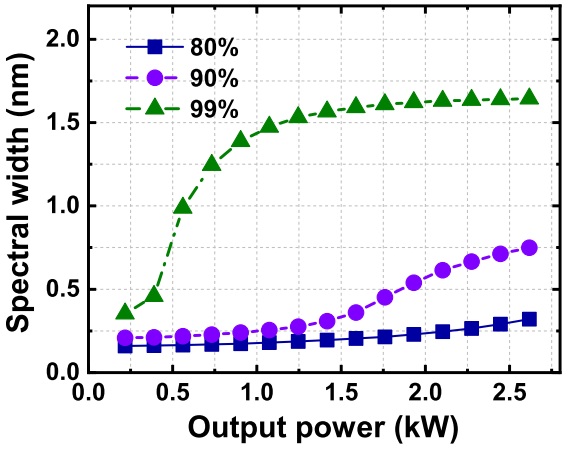

Fig. 3. Power-ratio spectral linewidths of total signal laser at different output powers.

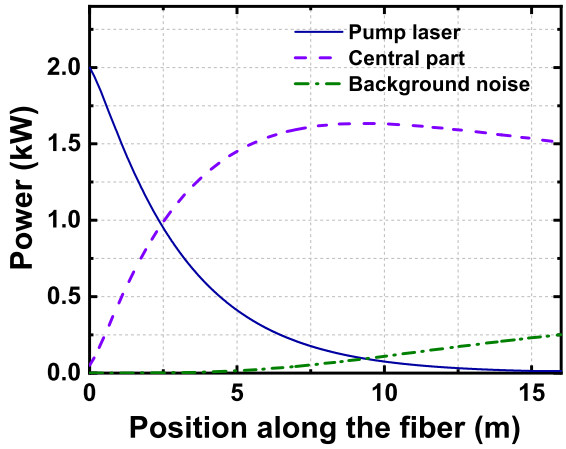

Fig. 4. Power evolutions of the two spectral components along the fiber amplifier.

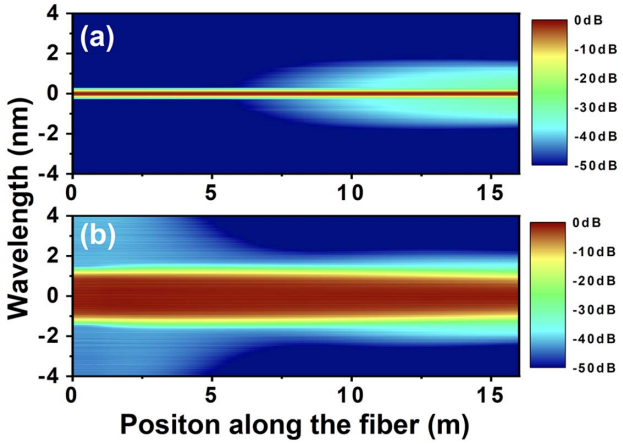

Fig. 5. Normalized spectral evolutions along the fiber amplifier: (a) the phase-modulated single-frequency part; (b) the background spectral noise.

the initial inserted seed laser; thus, the gain competition between them would not lead to obvious enhancement of the background spectral noise. Therefore, it could be inferred that obvious energy conversion occurs between the phase-modulated single-frequency part and the background spectral noise during amplification, which finally leads to the spectral wing broadening in narrow-linewidth fiber lasers.

Apart from gain competition, the FWM effect could also lead to energy conversion between the two different spectral components. To further clarify the energy conversion between the phase-modulated single-frequency part and the background spectral noise, we conduct contrast simulations by ignoring the FWM terms $A_1A_1A_0^*$ and $A_0A_0A_1^*$ in the simulation. Figure 6 illustrates the output spectrum of the total signal laser at a pump power of 2 kW when ignoring the FWM terms in the simulation. As shown in Fig. 6, the output spectrum of the total signal laser is similar to that of the total seed laser. In addition, the powers of the phase-modulated single-frequency part and the background spectral noise at the output port are about 1.76 kW and 1.75 W, respectively. Thus, the power ratio of the background spectral noise remains around

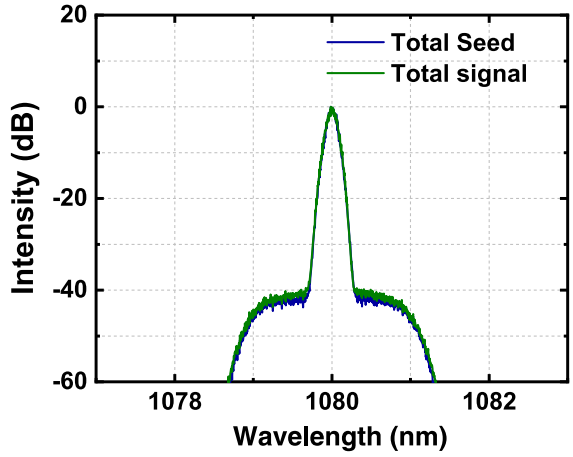

Fig. 6. Output spectrum of the total signal laser at a pump power of 2 kW when ignoring FWM terms in the simulation.

−30 dB when ignoring the FWM terms in the simulation. Therefore, it is the FWM effect that transfers energy from the phase-modulated single-frequency part into the background spectral noise and leads to the spectral wing broadening in narrow-linewidth YDFAs.

C. Design Strategies to Suppress Spectral Wing Broadening

According to the above analysis, two types of strategies could be applied to suppress the spectral wing broadening effect in narrow-linewidth fiber amplifiers, i.e., to optimize the properties of the background spectral noise in the phase-modulated single-frequency seed laser or to suppress the FWM effect in the fiber amplifier. The background spectral noise in phase-modulated single-frequency seed laser could be optimized through filtering out part of the background spectral noise. In this way, both the power ratio and bandwidth of the background spectral noise would be changed. Here we analyze the impact of the power ratio and bandwidth of the background spectral noise on the spectral wing broadening effect separately.

Figure 7(a) illustrates the power-ratio spectral linewidths of the total signal laser at a pump power of 2 kW, when the bandwidth of the background spectral noise is set to be 2 nm and its power ratio is different. As shown in Fig. 7(a), the power-ratio spectral linewidths of the total signal laser would first decrease and then remain nearly unchanged with the decrease of the power ratio of the background spectral noise. Specifically,

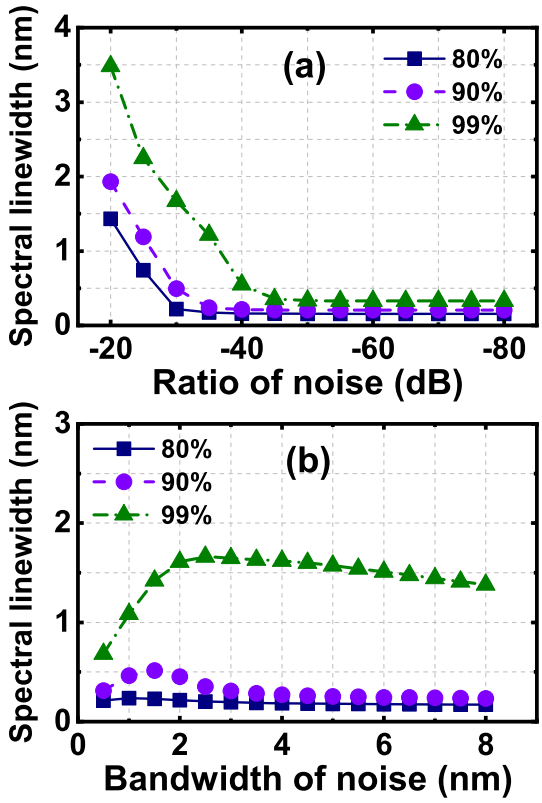

Fig. 7. Power-ratio spectral linewidths of the total signal laser at a pump power of 2 kW when the power ratio or the bandwidth of the background spectral noise is different: (a) the power ratio is different; (b) the bandwidth is different.

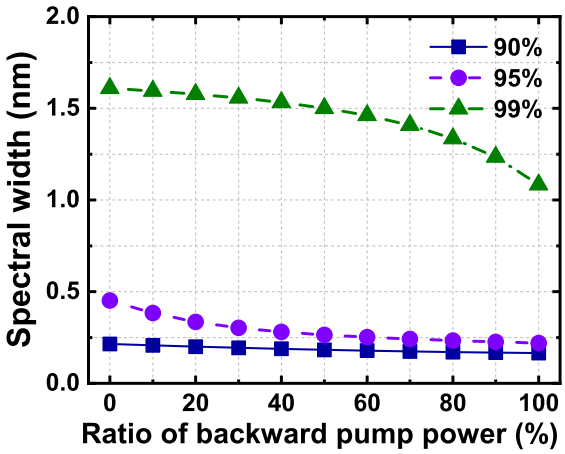

Fig. 8. Power-ratio spectral linewidths of the total signal laser at a pump power of 2 kW when the power ratio of the backward pump power is different.

the 99% power-ratio spectral linewidth of the total signal laser remains about 0.33 nm when the power ratio of the background spectral noise is below −50 dB, which is similar to that of the total seed laser. Therefore, the spectral wing broadening effect is effectively suppressed here. Figure 7(b) illustrates the power-ratio spectral linewidths of the total signal laser at a pump power of 2 kW, when the power ratio of the background spectral noise is set to be −30 dB and its bandwidth is different. As shown in Fig. 7(b), the power-ratio spectral linewidths would first increase and then decrease with the increase of the bandwidth of the background spectral noise. The maximum 80%, 90%, and 99% power-ratio spectral linewidths occur in the cases when the bandwidths of the background spectral noise are set to be about 1.0, 1.5, and 2.5 nm, respectively. Accordingly, it could be speculated that the background spectral noise at a specific band would have more significant impact on the spectral wing broadening effect. Therefore, filtering out the background spectral noise at specific band would be beneficial to control the spectral purity of the total signal laser.

The FWM effect could be suppressed through optimizing the pump configuration to reduce the average power of the signal laser along the fiber amplifier. Figure 8 illustrates the power-ratio spectral linewidths of the total signal lasers at a pump power of 2 kW, when the power ratio of the backward pump power is different. As shown in Fig. 8, the 80%, 90%, and 99% power-ratio spectral linewidths decrease gradually from about 0.21, 0.45, and 1.61 nm to about 0.17, 0.22, and 1.08 nm, respectively, when the power ratio of the backward pump power increases from 0% (co-pumped configuration) to 100% (counter-pumped configuration). Therefore, through applying a counter-pumped configuration, the spectral wing broadening effect could be partially suppressed in narrow-linewidth fiber amplifiers based on phase-modulated single-frequency seed lasers.

4. EXPERIMENTAL VALIDATION

To validate the theoretical model and the design strategies to suppress the spectral wing broadening effect, a high-power narrow-linewidth fiber amplifier system is established. Figure 9 illustrates the experimental setup of the all-fiber amplifier system. The seed laser is a phase-modulated single-frequency laser (PM-SF) with central wavelength of about 1081 nm, which mainly consists of a single-frequency master oscillator, a white-noise-signal phase modulation module, a 5 W commercial preamplifier, and a 40 W power-level preamplifier. The output power of the seed laser is about 40 W. The seed laser passes through a band-pass filter (BPF) to filter out part of the background spectral noise. Through changing the bandwidth of the BPF, the power ratio and the bandwidth of the background spectral noise can be partially controlled. A mode field adaptor (MFA) is utilized to improve the coupling between the seed laser and the main amplifier. The main amplifier consists of Yb-doped fiber (YDF), two pump combiners, two cladding light strippers (CLSs), and a quartz beam hat (QBH). The double-clad active fiber has a core diameter of 20 μm and an inner cladding diameter of 400 μm. The cladding absorption coefficient of the active fiber is about 1.2 dB/m at 976 nm, and 16 m active fiber is used in the main amplifier. About 3 m double-clad passive fiber with the same core and inner cladding diameters is spliced to the active fiber for power delivery. The CLSs are utilized to remove unwanted cladding light. The high-power laser diodes (LDs) with 976 nm central wavelength are divided into two groups to realize co-pumped and counter-pumped configurations, respectively.

We first apply the BPF with the bandwidth of 8 nm and co-pumped configuration to demonstrate the spectral wing broadening effect and verify the theoretical model. Figures 10(a)–10(d) compare the normalized measured and simulated spectra of the total seed laser and the total signal lasers when the output powers are 0.48, 0.99, and 1.51 kW, respectively. Here the simulated spectrum of the total seed laser in Fig. 10(a) is constructed according to the measured spectrum of the total seed laser, and the simulated spectra of the total signal lasers are calculated based on the simulated spectrum of the total seed laser and the simulation parameters according to the experimental setup. As shown in Figs. 10(a)–10(d), there exists an obvious spectral wing broadening phenomenon in this narrow-linewidth fiber amplifier with increasing output power. In addition, the simulated spectra of the total signal lasers are identical to the measured ones. Therefore, there could exist a spectral wing broadening effect in narrow-linewidth fiber amplifiers based on phase-modulated single-frequency seed lasers with background spectral noise, and our proposed theoretical model could describe this phenomenon effectively.

We also conduct contrast experiments through changing the bandwidth of the BPF or applying a counter-pumped configuration to validate the design strategies for high-spectral-purity operation. Figure 11 illustrates the 99% power-ratio spectral

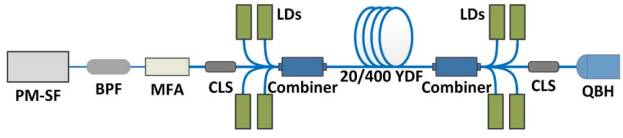

Fig. 9. Experimental setup of the fiber amplifier.

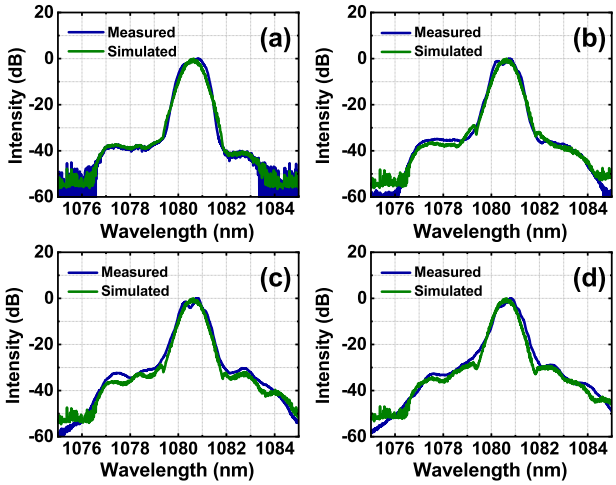

Fig. 10. Normalized measured and simulated spectra of the fiber amplifier at different output powers: (a) seed laser; (b) 0.48 kW; (c) 0.99 kW; (d) 1.51 kW.

linewidths of the total signal laser at different output powers when the experimental setups are different. As shown in Fig. 11, when applying the BPF with the bandwidth of 8 nm and the co-pumped configuration, the 99% power-ratio spectral linewidths of the total signal laser grow with the output power. The 99% power-ratio spectral linewidth at an output power of 1.51 kW is about 2 nm, which corresponds to a spectral broadening factor of about 1.3. However, when applying the BPF with the bandwidth of 8 nm and the counter-pumped configuration, the 99% power-ratio spectral linewidth remains around 1.5 nm at different output powers. Therefore, the spectral wing broadening effect in this narrow-linewidth fiber amplifier could be effectively suppressed through applying a counter-pumped configuration. When applying the BPF with the bandwidth of 2 nm, the 99% power-ratio spectral linewidth is always smaller than that in the cases when applying the BPF with the bandwidth of 8 nm at an output power below 1.28 kW. Thus, the spectral wing broadening effect in this narrow-linewidth fiber amplifier could also be suppressed through

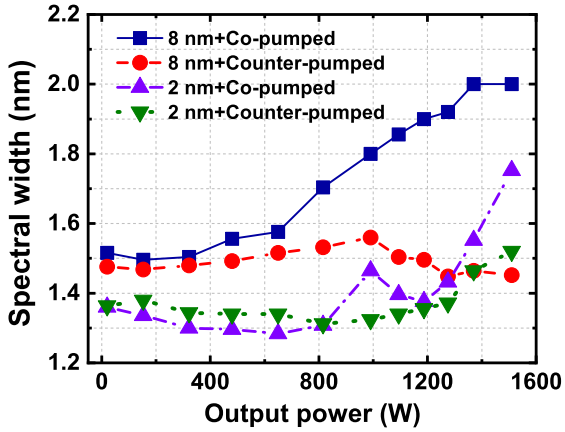

Fig. 11. Ninety-nine percent power-ratio spectral linewidths of the total signal laser at different output powers when the experimental setups are different.

filtering out the background spectral noise in the seed laser. However, when the output power is over 1.28 kW, the 99% power-ratio spectral linewidth increases quickly and even exceeds the case when applying the BPF with the bandwidth of 8 nm and the counter-pumped configuration. A possible explanation for this result is that the spectral filtering process could also lead to the degeneration of the temporal stability of the seed laser, especially for the case when the energy conversion between the central phase-modulated single-frequency part and the background noise has occurred effectively in the preamplifiers. Therefore, the bandwidth of the BPF should be carefully designed to both filter out the background spectral noise as much as possible and to avoid the degeneration of the temporal stability of the seed laser.

5. CONCLUSIONS

In this work, we propose a spectral evolution model for narrow-linewidth fiber amplifiers to analyze the effects of the background spectral noise in the phase-modulated single-frequency seed laser on the spectral purity of the signal laser. Through demonstrating the spectral evolutions of the phase-modulated single-frequency part and the background spectral noise, the interactions between the two spectral components are given. The theoretical results clarify that it is the FWM effect that transfers energy from the phase-modulated single-frequency part into the background spectral noise and leads to the spectral wing broadening in narrow-linewidth YDFAs. Accordingly, the spectral wing broadening effect could be suppressed by filtering out the background spectral noise in the seed laser or applying a counter-pumped configuration in the YDFAs. We have also conducted contrast experiments, which have verified the validity of the theoretical model and the design strategies for high-spectral-purity operation. We believe that this work could provide a good reference for improving the spectral purity of high-power narrow-linewidth fiber lasers.

Funding. National Natural Science Foundation of China (62005313, 61705264); Innovative Research Team in Natural Science Foundation of Hunan Province (2019JJ10005); Hunan Provincial Innovation Construct Project (2019RS3017); Guangdong Key Research and Development Program (2018B090904001).

Disclosures. The authors declare no conflicts of interest.

REFERENCES

1. D. J. Richardson, J. Nilsson, and W. A. Clarkson, "High power fiber lasers: current status and future perspectives [Invited]," J. Opt. Soc. Am. B **27**, B63–B92 (2010).
2. M. N. Zervas and C. A. Codemard, "High power fiber lasers: a review," IEEE J. Sel. Top. Quantum Electron. **20**, 0904123 (2014).
3. W. Shi, Q. Fang, X. Zhu, R. A. Norwood, and N. Peyghambarian, "Fiber lasers and their applications [Invited]," Appl. Opt. **53**, 6554–6568 (2014).
4. H. Grote, "Overview and status of advanced interferometers for gravitational wave detection," J. Phys. Conf. Ser. **718**, 022009 (2016).
5. W. D. Jay, J. M. Michael, J. B. Raymond, Y. S. Miroslav, A. S. Eddy, K. S. Arun, H. P. Paul, E. H. John, W. S. Craig, and C. P. J. Barty, "Analysis of the scalability of diffraction-limited fiber lasers and amplifiers to high average power," Opt. Express **16**, 13240–13266 (2008).

6. J. Zhu, P. Zhou, Y. Ma, X. Xu, and Z. Liu, "Power scaling analysis of tandem-pumped Yb-doped fiber lasers and amplifiers," Opt. Express **19**, 18645–18654 (2011).
7. J. Ballato, H.-J. Otto, C. Jauregui, J. Limpert, and A. Tünnermann, "Average power limit of fiber-laser systems with nearly diffraction-limited beam quality," Proc. SPIE **9728**, 97280E (2016).
8. M. N. Zervas, "Transverse mode instability, thermal lensing and power scaling in Yb^{3+}-doped high-power fiber amplifiers," Opt. Express **27**, 19019–19041 (2019).
9. Q. Chu, Q. Shu, Z. Chen, F. Li, D. Yan, C. Guo, H. Lin, J. Wang, F. Jing, C. Tang, and R. Tao, "Experimental study of mode distortion induced by stimulated Raman scattering in high-power fiber amplifiers," Photon. Res. **8**, 595–600 (2020).
10. T. Y. Fan, "Laser beam combining for high-power, high-radiance sources," IEEE J. Sel. Top. Quantum Electron. **11**, 567–577 (2005).
11. C. Wirth, O. Schmidt, I. Tsybin, T. Schreiber, R. Eberhardt, J. Limpert, A. Tünnermann, K. Ludewigt, M. Gowin, E. T. Have, and M. Jung, "High average power spectral beam combining of four fiber amplifiers to 8.2 kW," Opt. Lett. **36**, 3118–3120 (2011).
12. Z. Liu, P. Ma, R. Su, R. Tao, Y. Ma, X. Wang, and P. Zhou, "High-power coherent beam polarization combination of fiber lasers: progress and prospect [Invited]," J. Opt. Soc. Am. B **34**, A7–A14 (2017).
13. Y. Zheng, Y. Yang, J. Wang, M. Hu, G. Liu, X. Zhao, X. Chen, K. Liu, C. Zhao, B. He, and J. Zhou, "10.8 kW spectral beam combination of eight all-fiber superfluorescent sources and their dispersion compensation," Opt. Express **24**, 12063–12071 (2016).
14. J. Xu, L. Huang, M. Jiang, J. Ye, P. Ma, J. Leng, J. Wu, H. Zhang, and P. Zhou, "Near-diffraction-limited linearly polarized narrow-linewidth random fiber laser with record kilowatt output," Photon. Res. **5**, 350–354 (2017).
15. J. Lee, K. H. Lee, H. Jeong, M. Park, J. H. Seung, and J. H. Lee, "2.05 kW all-fiber high-beam-quality fiber amplifier with stimulated Brillouin scattering suppression incorporating a narrow-linewidth fiber-Bragg-grating-stabilized laser diode seed source," Appl. Opt. **58**, 6251–6256 (2019).
16. Y. Xu, Q. Fang, Y. Qin, X. Meng, and W. Shi, "2 kW narrow spectral width monolithic continuous wave in a near-diffraction-limited fiber laser," Appl. Opt. **54**, 9419–9421 (2015).
17. M. Jiang, P. Ma, L. Huang, J. Xu, P. Zhou, and X. Gu, "kW-level, narrow-linewidth linearly polarized fiber laser with excellent beam quality through compact one-stage amplification scheme," High Power Laser Sci. Eng. **5**, e30 (2017).
18. Y. Huang, P. Yan, Z. Wang, J. Tian, D. Li, Q. Xiao, and M. Gong, "2.19 kW narrow linewidth FBG-based MOPA configuration fiber laser," Opt. Express **27**, 3136–3145 (2019).
19. A. Flores, C. Robin, A. Lanari, and I. Dajani, "Pseudo-random binary sequence phase modulation for narrow linewidth, kilowatt, monolithic fiber amplifiers," Opt. Express **22**, 17735–17744 (2014).
20. Y. Roman, P. Nikolai, Y. Alexander, and P. G. Valentin, ">1.5 kW narrow linewidth CW diffraction-limited fiber amplifier with 40 nm bandwidth," Proc. SPIE **9728**, 972807 (2016).
21. P. Ma, R. Tao, R. Su, X. Wang, P. Zhou, and Z. Liu, "1.89 kW all-fiberized and polarization-maintained amplifiers with narrow linewidth and near-diffraction-limited beam quality," Opt. Express **24**, 4187–4195 (2016).
22. W. Liu, P. Ma, H. Lv, J. Xu, P. Zhou, and Z. Jiang, "General analysis of SRS-limited high-power fiber lasers and design strategy," Opt. Express **24**, 26715–26721 (2016).
23. W. Liu, P. Ma, P. Zhou, and Z. Jiang, "Spectral property optimization for a narrow-band-filtered superfluorescent fiber source," Laser Phys. Lett. **15**, 025103 (2018).
24. F. Beier, C. Hupel, S. Kuhn, S. Hein, J. Nold, F. Proske, B. Sattler, A. Liem, C. Jauregui, J. Limpert, N. Haarlammert, T. Schreiber, R. Eberhardt, and A. Tunnermann, "Single mode 4.3 kW output power from a diode-pumped Yb-doped fiber amplifier," Opt. Express **25**, 14892–14899 (2017).
25. T. Li, C. Zha, Y. Sun, Y. Ma, W. Ke, and W. Peng, "3.5 kW bidirectionally pumped narrow-linewidth fiber amplifier seeded by white-noise-source phase-modulated laser," Laser Phys. **28**, 105101 (2018).
26. P. Ma, H. Xiao, D. Meng, W. Liu, R. Tao, J. Leng, Y. Ma, R. Su, P. Zhou, and Z. Liu, "High power all-fiberized and narrow-bandwidth MOPA system by tandem pumping strategy for thermally induced mode instability suppression," High Power Laser Sci. Eng. **6**, e57 (2018).
27. H. Lin, R. Tao, C. Li, B. Wang, C. Guo, Q. Shu, P. Zhao, L. Xu, J. Wang, F. Jing, and Q. Chu, "3.7 kW monolithic narrow linewidth single mode fiber laser through simultaneously suppressing nonlinear effects and mode instability," Opt. Express **27**, 9716–9724 (2019).
28. W. Liu, P. Ma, H. Lv, J. Xu, P. Zhou, and Z. Jiang, "Investigation of stimulated Raman scattering effect in high-power fiber amplifiers seeded by narrow-band filtered superfluorescent source," Opt. Express **24**, 8708–8717 (2016).